

A.S.FOUDA, G.Y.ELEWADY
M.G. SALAMA

Scientific paper
UDC:620.173:669.75'782

Corrosion inhibition of aluminum-silicon alloy in H_2SO_4 solution using some thiophene derivatives

Inhibition of corrosion of Al-Si alloy by some thiophene derivatives in 0.5M H_2SO_4 was investigated by potentiodynamic polarization and electrochemical impedance spectroscopy (EIS) techniques. Polarization studies were carried out at different temperatures and showed that the investigated compounds are anodic inhibitors. The effect of temperature on corrosion inhibition has been studied and thermodynamic activation and adsorption parameters were calculated and discussed. Electrochemical impedance was used to investigate the mechanism of corrosion inhibition. The inhibition occurs through adsorption of the investigated compounds on the alloy surface without modifying the mechanism of corrosion process. The experimental data fit both of Temkin and kinetic-thermodynamic isotherm. A clear correlation was found between corrosion inhibition efficiency and theoretical parameters obtained by PM3 semiempirical method. The experimental results are supported by the theoretical data.

Keywords: Thiophene derivatives; corrosion inhibition; Al-Si alloy; H_2SO_4 , quantum chemical calculations.

1. INTRODUCTION

Aluminum and its alloys are widely used because of their appearance, low density and corrosion resistance. Nevertheless sometimes additional protection is required. Then, aluminum alloys can be easily protected with organic coatings by electrochemical oxidation. The latter generates oxide passive layers providing excellent corrosion resistance in highly aggressive environments. However, due to different thermomechanical treatments applied to achieve the mechanical properties, they are liable to suffer from various forms of corrosion, mainly pitting and intergranular attack [1-2]. Aluminum alloys are important structural metals, particularly in the aerospace industry. Pure aluminum metal (without alloying elements) is rather corrosion resistant, a result of passive film that forms on the metal surface. However, pure aluminum metal does not possess adequate strength for most aerospace application and must be alloyed with other metals, notably copper, magnesium, silicon, iron, zinc and other minor constituent. These alloys are classified by a numbering system that reflects both the chemical composition and the heat treatment (tempering) of the alloy [3-4]. The use of organic compounds as corrosion inhibitors for Al and Al alloys in HCl and H_2SO_4 acids have been the object of large number of investigators [5-18].

The present work was designed to study the corrosion inhibition of Al-Si alloy in H_2SO_4 solutions by some thiophene derivatives as corrosion inhibitors using different techniques. The synergistic effect brought about by combination of the inhibitors with $LaCl_3$ was examined also and explained.

2. MATERIALS AND METHODS

2.1. Materials and solutions

The aluminum-silicon alloy which employed for this study has a composition 89.15% Al and 10.85% Si. A

cylindrical alloy rod whose exposed surface was 1 cm^2 was inserted into a Teflon tube so that only the flat surface was in contact with solution. Before each experiment, the electrode was abraded with a sequence of emery papers of different grades (600, 800, 1200), washed with double distilled water and degreased with acetone. All chemicals used were of analytical-grade reagents. Solutions were prepared with double distilled water. The corrosive solution was 0.5 M sulfuric acid and prepared using double distilled water. The experiments were carried out under non-stirred and naturally aerated conditions. The inhibitor solutions were prepared at different concentrations using absolute ethanol.

2.2 Inhibitors

The selected organic inhibitors used in this study were synthesized through procedures reported previously [19]. The structure formulae of inhibitors are shown in Fig. 1.

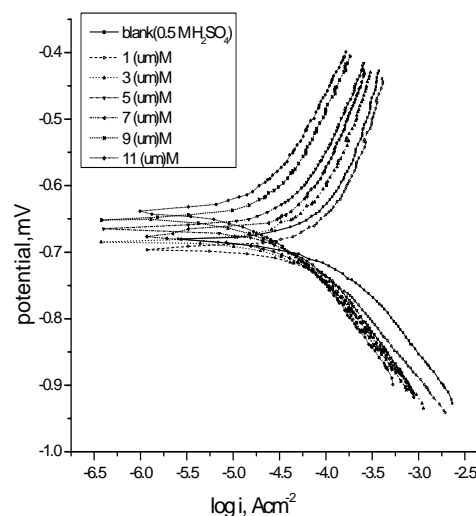
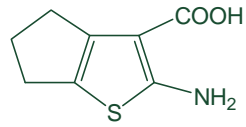
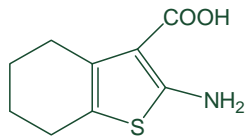
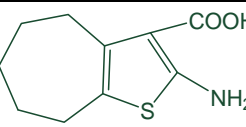


Fig. 1 - Potentiodynamic curves for the Al-Si alloy in 0.5M of H_2SO_4 in the presence and absence of different concentrations of compound A at 25°C

Address author: Chemistry Department, Faculty of Science, El-Mansoura University, El-Mansoura-35516, Egypt. email. asfouda@mans.edu.eg

No.	Name	Structure	Mol. Wt.
(A)	2-amino-5,6-dihydro-4H-cyclopenta[b]thiophene-3-carboxylic acid		183
(B)	2-amino-4,5,6,7-tetrahydrobenzo[b]thiophene-3-carboxylic acid		197
(C)	2-amino-5,6,7,8-tetrahydro-4H-cyclohepta[b]thiophene-3-carboxylic acid		211

2.2 Methods

2.2.1. Potentiodynamic polarization

Electrochemical experiments were performed in a conventional three-electrode electrochemical cell at 25 °C with a platinum counter electrode and saturated calomel (SCE) as reference electrode. The working electrode was in the form of disc cut from the alloy under investigation, first was immersed into the test solution for 30 min to establish a steady state open circuit potential.

The potentiodynamic current-potential curves were recorded by changing the electrode potential automatically from -250 mV to +250 mV with scanning rate of 5 mV s⁻¹ using Gamry framework instruments (version 3.20). Corrosion current densities (j_{corr}) and corrosion potential (E_{corr}), were evaluated from intersection of the linear anodic and cathodic branches of Tafel plots and all of them will be calculated in absence and presence of different concentrations of inhibitors. Experiments were always repeated at least three times. Degree of surface coverage (θ) is calculated, as proposed by Vracar and Drazic [20], from the following equation:

$$\theta = (j_{corr} - j'_{corr})/j_{corr} \quad (1)$$

and % IE were calculated using the following equation:

$$\% IE = \theta \times 100 \quad (2)$$

where j_{corr} and j'_{corr} are the current densities in the absence and presence of inhibitors, respectively and θ is surface coverage.

2.2.2. Electrochemical impedance spectroscopy

Electrochemical impedance spectroscopy were performed at corrosion potentials, E_{corr} , over a frequency range of 10⁻⁵ Hz to 0.5 Hz with a signal amplitude perturbation of 10 mV, using potentiostat/galvanostat (Gamry PCI 300/4) and personal computer with EIS300 software for calculations. Data were presented as Nyquist and Bode plots. Experiments were always repeated at

least three times. Degree of surface coverage (θ) and % IE were calculated using the following equations:

$$\theta = [(1/R'_{ct}) - (1/R_{ct})] / (1/R'_{ct}) \quad (3)$$

$$\% IE = \theta \times 100 \quad (4)$$

where R'_{ct} and R_{ct} are the charge transfer resistance in the presence and absence of inhibitor, respectively.

2.3. Quantum calculations

Materials studio V.4.4.0 was used for molecular modeling. The molecular orbital calculation are based on a semiempirical self-consistent field molecular orbital (SCF-MO) method. A full optimization of all geometrical variables without any symmetry constraints was performed at the restricted Hartree-Fock (RHF) level using Parameterization Model 3 (PM3) method.

3. RESULTS AND DISCUSSION

3.1 Potentiodynamic polarization measurements

Figure (1) shows both the cathodic and anodic polarization curves of Al-Si alloy in the presence and absence of different concentrations of compound (C). Similar curves were obtained for the other compounds (not shown). Table (1) shows the electrochemical parameters of corrosion potential (E_{corr}), corrosion current densities (j_{corr}), cathodic and anodic Tafel slopes (β_c & β_a), the degree of surface coverage (θ), percentage inhibition efficiency (% IE) and corrosion rate (CR). The data show that the corrosion current density (j_{corr}) decreases with increasing the concentration of inhibitors. The order of decreasing the values of (j_{corr}) and hence the rate of corrosion is as follows: A > B > C. The slopes of the anodic (β_a) and cathodic (β_c) Tafel lines remain almost constant upon increasing inhibitor concentrations. These results indicate that these inhibitors act by blocking the available surface area [21]. In other words, these inhibitors decrease the surface area for corrosion without affecting the mechanism of corrosion and only cause inactivation of a part of metal surface with respect to the

corrosive medium. The slight shift of corrosion potential (E_{corr}) values towards less negative direction by increase of the inhibitor concentrations in the presence of 0.5 M

H_2SO_4 indicates that these investigated compounds are anodic inhibitors [22].

Table 1 - The effect of concentration of the investigated compounds on the free corrosion potential (E_{corr}), corrosion current density (j_{corr}), Tafel slopes (β_a & β_c), inhibition efficiency (% IE), degree of surface coverage (θ) and corrosion rate (CR) for the corrosion of Al-Si alloy in H_2SO_4 at 25 °C

compounds	Conc. μM	$-E_{\text{corr}}$ mV	j_{corr} $\mu\text{A cm}^{-2}$	β_a mVdec $^{-1}$	β_c mVdec $^{-1}$	θ	% IE	CR mm y^{-1}
Free acid	0.0	732	161.9	179	466	----	----	1.795
(A)	1	697	94.88	186	366	0.413	41.3	1.031
	3	685	82.26	217	429	0.492	49.2	0.894
	5	664	56.70	201	375	0.650	65.0	0.616
	7	677	39.81	170	282	0.754	75.4	0.433
	9	652	31.77	181	327	0.804	80.4	0.345
	11	640	28.23	192	320	0.826	82.6	0.307
(B)	1	707	118.9	123	525	0.271	27.1	1.292
	3	690	104.7	222	546	0.353	35.3	1.138
	5	644	67.65	212	414	0.582	58.2	0.735
	7	674	49.66	200	359	0.693	69.3	0.540
	9	642	32.53	188	308	0.799	79.9	0.353
	11	646	29.91	191	296	0.815	81.5	0.325
(C)	1	749	147.3	181	461	0.090	9.0	1.600
	3	744	110.8	164	351	0.315	31.5	1.204
	5	751	99.25	179	387	0.387	38.7	1.079
	7	761	74.83	157	313	0.538	53.8	0.813
	9	672	50.54	195	333	0.688	68.8	0.549
	11	655	39.64	187	308	0.755	75.5	0.431

From the calculated values of (% IE) at 25 °C as shown in Table (2), the order of decreasing the inhibition efficiency of the investigated compounds is as follows: A > B > C

Table 2 - Inhibition efficiency at different concentration of the investigated compounds for the corrosion of Al-Si alloy in 0.5M H_2SO_4 at 25 °C.

Concentration, μM	IE %		
	(A)	(B)	(C)
1	41.3	27.1	9.0
3	49.2	35.3	31.5
5	65.0	58.2	38.7
7	75.4	69.3	53.8
9	80.4	79.9	68.8
11	82.6	81.5	75.5

3.2 Electrochemical impedance spectroscopy

The corrosion behavior of Al-Si alloy in 0.5 M H_2SO_4 in the presence and absence of investigated thiophene derivatives was investigated by (EIS) at 25 °C. Various impedance parameter such as charge transfer resistance (R_{ct}), double layer capacitance (C_{dl}) and inhibition efficiency (% IE) were calculated and are given in Table (3). The data obtained show that (R_{ct}) charge transfer resistance increases with increasing the concentration of inhibitors which accompanied with increasing (% IE) and the value of capacitance double layer (C_{dl}) decrease with increasing the concentration of inhibitor due to the adsorption of these compound on the electrode surface leading to a film formation of Al-Si alloy surface.

Table 3 - Electrochemical kinetic parameter obtained by EIS technique for the corrosion of Al-Si alloy in 0.5M H_2SO_4 at different concentration of investigated compound.

Compounds	Concentration μM	C_{dl} , $\mu\text{F cm}^{-2}$	R_{ct} , $\Omega \text{ cm}^2$	Θ	% IE
blank	0.0	27.91	122.9	0	0.0
A	5	24.72	160.9	0.236	23.6
	7	20.26	179.4	0.315	31.5
	9	16.52	202.8	0.394	39.4
	11	6.348	237.3	0.482	48.2
B	5	25.31	155.1	0.208	20.8
	7	21.02	174.3	0.295	29.5
	9	14.11	199.2	0.383	38.3
	11	8.09	226.5	0.457	45.8
C	5	24.96	149.9	0.180	18.0
	7	23.35	165.0	0.255	25.5
	9	17.42	178.9	0.314	31.4
	11	11.52	211.7	0.42	42.0

The obtained Nyquist impedance diagram in most cases does not show perfect semicircle. This may be attributed to the frequency dispersion as a result of the heterogeneity of the electrode surface [23-24].

In 0.5 M H_2SO_4 and presence of various concentrations of investigated inhibitors, the impedance diagram shows the same trend. However, the diameters of the capacitive loop increase with increasing concentration of the inhibitor. Fig (2) shows the Nyquist plot for Al-Si alloy in 0.5 M H_2SO_4 in the absence and presence of different concentrations of compound (A) at 25 °C.

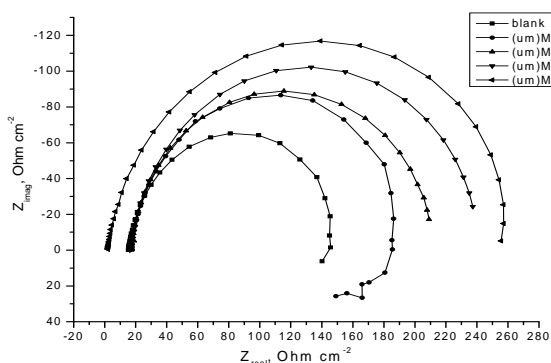


Fig. 2 - The Nyquist plot for Al-Si alloy in 0.5 M H_2SO_4 solution in the absence and presence of different concentration of compound (A) at 25 °C

This diagram has a semicircle appearance; it indicates that the corrosion of Al-Si alloy is mainly controlled by a charge transfer process. The Bode plot for the alloy is shown in Figure (3) where the high frequency limit corresponds to electrolyte resistance R_{Ω} , while the low frequency limit represents the sum of ($R_{\Omega} + R_p$) where R_p is the first approximation determined by both the electrolytic conductance of the oxide film and polarization resistance of the dissolution and repassivation process.

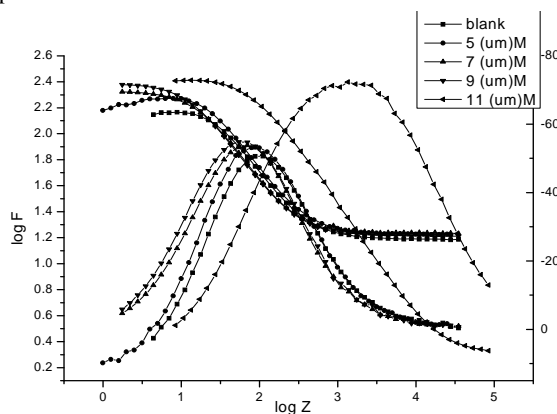


Fig. 3 - The bode plot for Al-Si alloy in 0.5 M H_2SO_4 solution in the absence and presence of different concentrations of compound (A) at 25 °C

3.3 Adsorption isotherm

The investigated compounds inhibit the corrosion by adsorption at the metal surface. Theoretically, the adsorption process has been regarded as a simple substitutional process, in which an organic molecule in the aqueous phase substitutes an (y) number of water molecules adsorbed on the metal surface [25].

A number of mathematical relationships for the adsorption isotherms have been suggested to fit the experimental data of the present work. The simplest equation is that due to Temkin [26] and is given by the general relation:

$$a\theta = KC \quad (5)$$

where K is the equilibrium constant of the adsorption reaction, C is the inhibitor concentration in the bulk of the solution.

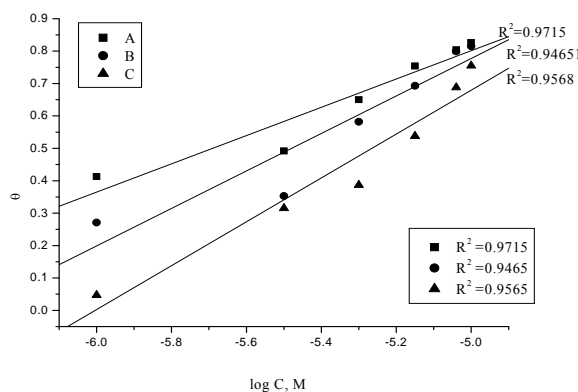


Fig. 4 - Temkin adsorption isotherm plotted as θ vs. $\log C$ of the investigated inhibitors for corrosion of Al-Si alloy in 0.5 M H_2SO_4 solution at 25 °C

Figure (4) shows relationship between θ and $\log C$ where K (equilibrium constant) is obtained from the intercept of the straight line and it is known that standard free energy (ΔG_{ads}°) is related to equilibrium constant by:

$$K = 1/55.5 \exp(-\Delta G_{ads}^\circ / RT) \quad (6)$$

The value of 55.5 is the concentration of water in the solution in mole per liter.

Also it is found that the kinetic thermodynamic model of El-awady et al [27] is fit well to the experimental data of Al-Si alloy in the presence of varying concentration of tested compounds in H_2SO_4 . The adsorption isotherm relationship is represented by the following equation:

$$\log(\theta / (1-\theta)) = \log K' + y \log C \quad (7)$$

where (y) is the number of inhibitor molecules occupying one active site, $K = K^{(1/y)}$ and (1/y) is the number of adsorbed water molecules replaced by one

molecules of organic inhibitor. Application of kinetic-thermodynamic equation yields a straight line with slope of (y) and intercept of $\log(K')$ illustrated in Fig.(5). The results in Table (4) show the values of ΔG_{ads}° , K and (1/y) obtained from El-Awady et al and Temkin's adsorption isotherm. Inspection of Table 4 shows that the number of active sites is nearly constant and approximately equals one, this behavior can be discussed on the basis that the adsorption process takes place by the occupation of one active site per single inhibitor molecules. Also, the equilibrium constant (K) decreases in the order: $A > B > C$. Large values of K mean better inhibition efficiency of a given inhibitors, i.e., strong electric interaction between the double layer existing at the phase boundary and the adsorbing molecules. The values of ΔG_{ads}° are large and acquire negative sign indicating that the adsorption reaction is proceeding spontaneously and accompanied with a high efficient adsorption for such compounds.

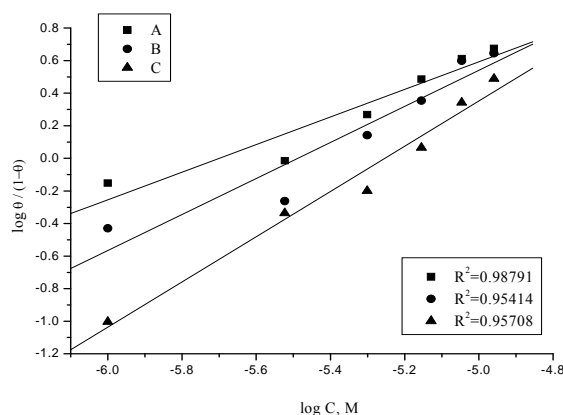


Fig. 5 - El-Awady model plotted as $\log(\theta/(1-\theta))$ vs. $\log C$ of the investigated inhibitors for corrosion of Al-Si alloy in 0.5 M H_2SO_4 solution at 25 °C.

According to Temkin model, the data (Table 4) indicate that the value of (K) decreases in the order: $A > B > C$. It is seen that there is a good agreement between the values of (K) and (ΔG_{ads}°) obtained from the kinetic model and Temkin model isotherm.

Table 4 - Equilibrium constant (K), adsorption free energy (ΔG_{ads}°) and number of active sites (1/y) for the adsorption of inhibitors of 11×10^{-6} on Al-Si alloy in 0.5 M H_2SO_4 at 25 °C

Inhibitor	Kinetic model			Temkin isotherm	
	1/y	$K \times 10^{-4}$ M ⁻¹	$-\Delta G_{ads}^\circ$ kJ mol ⁻¹	$K \times 10^{-4}$ M ⁻¹	$-\Delta G_{ads}^\circ$ kJ mol ⁻¹
A	1.18	50.11	42.48	686.12	48.96
B	0.90	30.79	41.27	220.90	46.15
C	0.72	17.96	39.93	100.88	44.21

3.4 Effect of temperature

Temperature has a significant influence on metals and alloys corrosion rates. In case of corrosion in an acidic medium, the corrosion rate increases with increase in temperature, because the decrease of hydrogen evolution overpotential [5]. An experimental dependence of Arrhenius-type equation on temperature is observed between the corrosion rate and temperature.

$$j_{corr} = A \exp(-E_a/RT) \quad (8)$$

and logarithmic form

$$\log j_{corr} = \log A - (E_a/2.303RT) \quad (9)$$

where j_{corr} is the corrosion current density, A is the extrapolation factor, E_a is the activation energy, R is the gas constant and T is the absolute temperature.

The effect of rising temperature on the corrosion rate of Al-Si alloy in 0.5 M H_2SO_4 solution in the absence and presence of 3×10^{-6} M of the investigated thiophene derivatives was studied by potentiodynamic polarization over a temperature range from 25- 40 °C. Corrosion rates in all systems increased to a great extent as temperature was raised from 25° to 40 °C. Also, investigated compounds are seen to maintain their inhibiting effect at all temperatures. The above observations can be explained with respect to the characteristic features of the cathodic process of hydrogen evolution, where the decrease of the reaction overpotential with rise in temperature leads to an increase in the rate of cathodic reaction [28]. The enhanced rates of hydrogen gas evolution will agitate the interface, which hinders inhibitor adsorption and also promotes dispersal of adsorbed inhibitor. Thus, the reduction in % IE with rise in temperature could be attributed to the shift of the adsorption-desorption equilibrium towards desorption. Such behavior suggests that investigated compounds were physically adsorbed on Al-Si alloy [29].

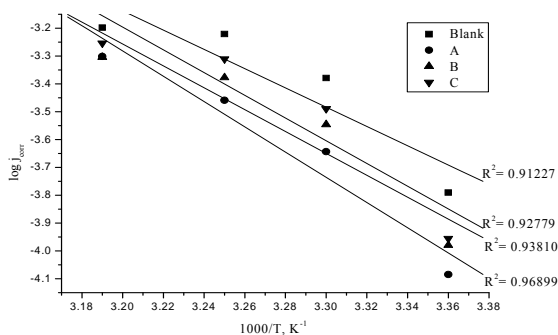


Fig. 6 - Arrhenius plots ($\log j_{corr}$ vs. $1/T$) for Al-Si alloy in 0.5 M H_2SO_4 in the absence and presence of $3 \mu M$ of investigated inhibitors

A plot of ($\log j_{corr}$ vs. $1/T$) gives straight lines with slope $E_a/2.303R$. The intercept be A. Fig.6 represents the

relation between log (rate) and reciprocal of the absolute temperature of Al-Si alloy in 0.5 M H_2SO_4 in the presence and absence of investigated compounds. The values of E_a are given in Table (5). Data of this Table reveal high activation energies for the inhibition process by different compounds, indicating their higher protective efficiency [22]. It is clear that the activation energy increases with increasing the efficiency of the investigated compounds in the following order: C < B < A. Such behavior is attributed to the formation of energy barrier, due to the adsorption of the inhibitors on the alloy surface forming a film. This is another pointer to inhibitor physisorption.

Table 5 - Thermodynamic activation parameters for Al-Si alloy dissolution in 0.5 M H_2SO_4 in absence and presence of 3×10^{-6} M of investigated inhibitors.

Inhibitor	E_a^* kJ mol ⁻¹	$H^*\Delta$ kJ mol ⁻¹	$S^*-\Delta$ J mol ⁻¹ K ⁻¹
Blank	66.3	63.8	101
A	86.9	76.2	64
B	78.2	75.9	66
C	75.3	72.8	74.7

An alternative formulation of arhenius equation is the transition state equation [30].

$$j_{corr} = RT/Nh \exp(\Delta S^*/R) \exp(-\Delta H^*/RT) \quad (10)$$

where h is the Planck's constant, N is Avogadro number, ΔS^* is the entropy change of activation and ΔH^* is the enthalpy change of activation. Figure (7) shows a plot of $\log(j_{corr}/T)$ against $(1/T)$ straight line are obtained with a slope of $(-\Delta H^*/2.303R)$ and intercept of $(\log R/Nh + \Delta S^*/2.303R)$ from which the value of ΔH^* & ΔS^* are calculated and are given in Table (5).

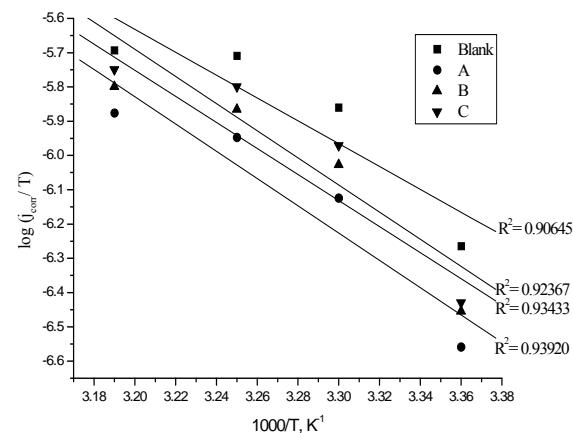


Fig. 7 - Arrhenius plots $\log j_{corr}/T$ vs. $(1/T)$ for Al-Si alloy in 0.5 M H_2SO_4 in the absence and presence of $3 \mu M$ of investigated inhibitors

From Table (5) it is clear that the positive value of ΔH^* reflects the endothermic nature of dissolution process. The Table also, shows that the presence of the inhibitor produces higher values for ΔH^* than those obtained for the uninhibited solution. This indicates higher protection efficiency. This may be attributed to the presence of an energy barrier for the reaction, that is, the process of adsorption leads to a rise in enthalpy of the corrosion process. In addition, the values of ΔS^* are large and negative. This implies that the activated complex in the rate determining step represents association rather than dissociation meaning that a decrease in disordering takes place on going from reactants to activated complex and the increase in the system order [31, 32].

3.5 Theoretical studies

To investigate the effect of ring structure on the inhibition mechanism and efficiency some quantum chemical calculations were performed.

Geometric and electronic structures of the inhibitors were calculated by optimization of their bond lengths and bond angles. The optimized molecular structures of the inhibitors are given in Fig.8b. Highest occupied molecular orbital (HOMO) and lowest unoccupied molecular orbital (LUMO) energies, LUMO-HOMO energy gap, dipole moment, μ , and inhibition efficiency are given in Table 6.

Table 6 - Quantum chemical parameter for investigated thiophene derivatives

PM3 liquid phase	-E _H eV	-E _L eV	ΔE eV	μ Debye
A	9.704	0.743	8.061	2.513
B	8.957	0.825	8.132	1.480
C	8.801	0.565	8.236	1.402

E_{HOMO} often is associated with the electron donating ability of the molecule. High values of E_{HOMO} are likely to indicate a tendency of the molecule to donate electrons to appropriate acceptor molecules with low energy, empty molecular orbitals. Therefore, the energy of the lowest unoccupied molecular orbitals indicates the ability of the molecule to accept electrons. The lower the value of E_{LUMO} , the most probable it is that the molecule accepts electron [33]. The percent inhibition efficiencies increase if the molecules have higher or less negative HOMO energies. The highest values of the HOMO density were found in the vicinity of sulphur and nitrogen atoms, clearly indicating the nucleophilic center is the sulphur and nitrogen atoms (Fig. 8a).

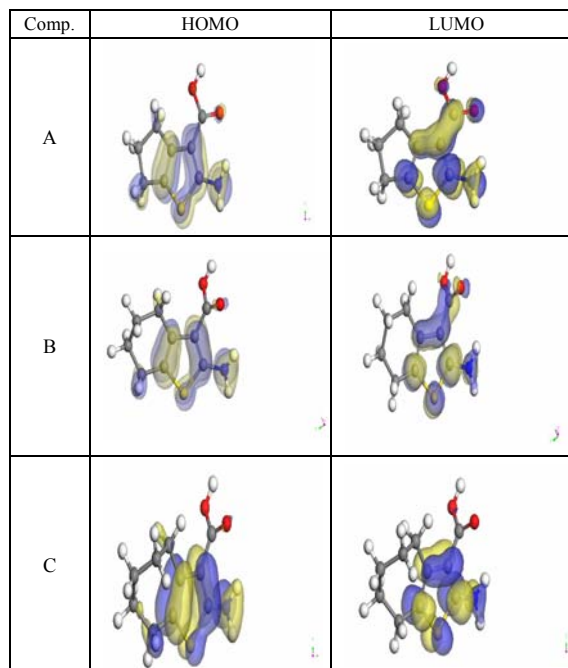
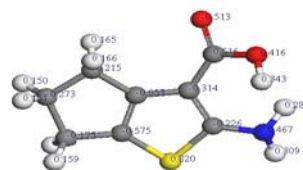
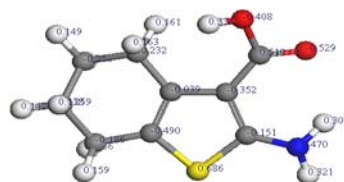


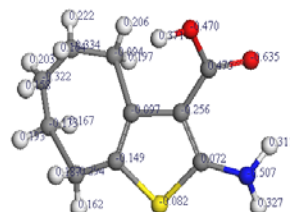
Fig. 8a - Optimized HOMO and LUMO structure of some thiophene derivatives



Compound A



Compound B



Compound C

Fig. 8b - Optimized molecular structure with Mulliken atomic charges of some thiophene derivatives

Table 6 shows the calculated values of dipole moment, μ , of the studied molecules. Highest dipole moment values were observed with compound (A). Other authors state that the inhibition efficiency increases with increasing value of the dipole moment [34] but on the other hand, a survey of literature reveals that irregularities appeared in the case of correlation of dipole moment with efficiency [35]. Also, from this Table the value of ΔE (energy gap) decreased when increasing the inhibition efficiency indicating that the more of inhibitors, the stronger interaction between inhibitors and metal surface. Thus, the interactions are probably physical adsorption, and the interactions between the inhibitors and the metal surface might be ascribed to the hyper conjugation interactions- π stacking [36].

As gathered from the higher values of E_{HOMO} , dipole moment and the lower values of E_{LUMO} the order on inhibition efficiency is as follows: $A > B > C$.

3.6. Mechanism of corrosion inhibition

Corrosion inhibition of aluminum-silicon alloy in H_2SO_4 solution by the investigated thiophene derivatives as indicated from potentiodynamic and impedance techniques was found to depend on the concentration and the nature of the inhibitor.

It is generally, assumed that adsorption of the inhibitor at the metal / solution interface is the first step in the action mechanism of the inhibitors in aggressive acid media. Four types of adsorption may take place during inhibition involving organic molecules at the metal / solution interface:

- 1) Electrostatic attraction between charged molecules and charged metal.
- 2) Interaction of unshared electrons pairs in the molecule with the metal.
- 3) Interaction of π electrons with the metal.
- 4) A combination of the above [37].

Concerning inhibitors, the inhibition efficiency depends on several factors; such as: (i) the number of adsorption sites and their charge density, (ii) molecular size, heat of hydrogenation, (iii) mode of interaction with the metal surface, and (iv) the formation metallic complexes [38]. Most organic inhibitors contain at least one polar group with an atom of nitrogen, sulfur or oxygen, each of them in principle representing an adsorption center. The inhibitive properties of such compounds depend on the electron densities surrounding the adsorption centers: the higher the electron density at the center, the more the effective the inhibitor.

In the aqueous acidic solutions, investigated compounds exist either as neutral molecules or in the form of cations (protonated). In general two modes of adsorption could be considered. The neutral form may adsorb on the alloy surface via the chemisorption mechanism, involving the displacement of water molecules from the metal surface and the sharing

electrons between the N, O, and S atoms and Al. The cationic form can also adsorb on the metal surface on the basis of donor-acceptor interactions between π -electrons of aromatic ring and vacant p-orbitals of Al. On the other hand, it is well known that the Al surface charges negative charge in acid solution [39, 40], so, the protonated investigated compounds may adsorb through electrostatic interactions between positively charged molecules and the negatively charged metal surface. When the protonated form is adsorbed on the metal surface, a coordinate bond may be formed by partial transference of electrons from N, O, and S atoms to the metal surface. In addition, owing to lone-pair electrons of N, O, and S atoms in the investigated compounds or the protonated form may combine with freshly generated Al^{3+} ions on Al surface forming metal inhibitor complexes. These complexes might get adsorbed onto Al surface by van der Waals force to form protective film which covers both anodic and cathodic reaction sites on the Al surface, and inhibits both reactions at the same time.

In the investigated thiophene derivatives the effective part in these molecules is the cyclopentane, cyclohexane and cycloheptane. As known from the stereo chemistry of these cycloalkanes the cyclopentane was found to lie flat completely on the alloy surface so, it covers larger areas of alloy surface than in case of cyclohexane and cycloheptane which are partially lie flat on the alloy surface. So, the inhibition efficiency of the investigated thiophene derivatives is as follows: $A > B > C$.

4. CONCLUSIONS

From the study the following conclusions can be made:

- i. Thiophene derivatives are good inhibitors of corrosion of Al-Si alloy in H_2SO_4 and inhibit the corrosion by being adsorbed onto the alloy surface.
- ii. The adsorption behavior of the inhibitors is consistent with Temkin adsorption model.
- iii. The mechanism of physical adsorption is applicable to the adsorption of the investigated thiophene derivatives on surface of Al-Si alloy.
- vi. The results of polarization indicated that these investigated compounds are of anodic inhibitors.
- v. As can be seen, good agreement between potentiodynamic polarization measurements, electrochemical impedance measurements and quantum chemical calculations is found.

5. REFERENCES

- [1] Davo, A. Conde, J.J. de Damborenea, Corros. Sci. 47 (2005) 1227.
- [2] H. Allachi, F. Chaouket, K. Draoui, J. Alloys and Compounds, 475 (2009) 300.
- [3] Hatch JE (ed), Aluminum: properties and physical metallurgy. American Society for Metals, Metals Park, (1984) 424.

- [4] D. E. Tallman, G. Spinks, A. Dominis, G. G. Wallace, J. Solid State Electrochem. 6 (2002) 73.
- [5] A. Popova, E. Sokolova, S. Raicheva, M. Christov, *corros. Sci.* 45 (2003) 33.
- [6] N.P. Zhuk, Course on Corrosion and Metal Protection, Metallurgy, (1976).
- [7] O.L. Riggs, R.M. Hurd, *Corrosion* 23 (1967) 252.
- [8] G. Perboni, G. Rocchini, Proceedings of 10th ICMC, Madras, (1988) 2763.
- [9] I.H. Omar, G. TrabANELLI, F. Zucchi, Proceedings of 10th ICMC, Madras, (1988) 2723.
- [10] B. Sanyal, K. Srivastava, *Br. Corros. J.* 9 (1974) 103.
- [11] R.P. Mathur, T. Vasudevan, *Corrosion* 38 (1982) 171.
- [12] I.A. Ammar, F.M. El Khorafi, *Werkstoffe and Korrosion* 24 (1973) 702.
- [13] F. Zucchi, G. TrabANELLI, Proceedings of the 7th European Symposium on Corrosion Inhibitors, Ferrara, (1990) 339.
- [14] O. Radovic, Proceeding of 2nd European Symposium on Corrosion Inhibitors, Ferrara, (1965) 178.
- [15] R.J Chin, K.Nobe, *J. Electrochem. Soc.* 119 (1972) 1457.
- [16] N.A. Darwish, F.Hilbert, W.J.Lorenz, H.Rosswang, *Electrochim. Acta* 18 (1973) 421.
- [17] E. McCafferty, N. Hackerman, *J. Electrochem. Soc.* 119 (1972) 999.
- [18] R. Hariharaputhran, N. Hackerman, A.A. Antony, P.M. Sanker, A. Gopalan, T. Vasudevan, I.S.
- [19] Vncatakrisna, *Br. Corros. J.* 33 (1998) 214.
- [20] D. Abd El-H Kader, M.Sc. Thesis, Mansoura Univeristy, Egypt, (2010).
- [21] Lj.Vracar and D.M.Drazie, *corros.Sci.*, 44(2002) 1669.
- [22] M.S.Abdel Aal, S.Radwan and A.Elsaied, *Brit.Corros.J.*, 18(1983)2.
- [23] E.E.Fouad El-Sherbini, S.M.Abd El-Wahab and M.A.Deyab, *Mater.Chem.Phys.*, 82(2003)631.
- [24] A.S. Fouda, G. Y. Elewady and K. Shalabi, *Mansoura J. of Chemistry*, 35(2) (2008) 23.
- [25] T. Paskossy, *J. Electroanal. Chem.* 364 (1994) 111.
- [26] Y.A. El-Awady and A.I. Ahmed, *Ind. J. Chem.*, 24A (1985) 601.
- [27] H.Dhar, B.Conway and K.Joshi, *Electrochim.Acta*, 18(1973)789.
- [28] Y.Harek and L.Larabi, *Kem.Ind.* 53 (2004) 55.
- [29] G.K.Gomma and M.H.Wahdan, *Bull.Chem.Soc.Jpn.*, 67 (1994)2621.
- [30] S. S. Al-Juaid, *Portugaliae Electrochimica Acta*, 25 (2007) 363.
- [31] S.A. Umoren, I.B. Obot, E.E. Ebenso, N.O. Obi-Egbedi, *Desalination* 247 (2009) 561.
- [32] A.Y. El-Etre, *Corros. Sci.* 45 (2003) 2485.
- [33] I.Lukovits, K.Palfi and E.Kalman, *Corrosion*, 53 (1997) 915.
- [34] A.Popova. M.Christov, S.Raicheva and E.Sokolova, *Corros.Sci.*, 46(2004)1333.
- [35] K.F.Kaled, K.Babic-Samardzic and N.Hackerman, *J.Appl.Electrochem.*, 34(2004)697.
- [36] P.M.Alvarez, J.F.Garacia-Araya, F.J.Beltran, F.J.Masa and F.Medina, *J.Colloid.Interface Sci.*, 283(2005)503.
- [37] S.Rajendran, *J.Electrochem.Soc.*, 54(2)(2005)61.
- [38] A.S.Fouda, M.M.Moussa, F.I.Taha and A.I.El-Neanaa, *Corros.Sci.*, 26(1986)719.
- [39] M.N.Desai, *Werkst.U.Korros.*, 23(1972)475
- [40] A.K.Vijh, *J.Phys.Chem.*, 72(1968)1148.
- [41] K. Vaso, M. Dema, J. Marku, Improvement of the physico-chemical characteristics of sunflower oil through thermo-chemical processing and its use in the anticorrosive paints, *Časopis „Zaštita materijala“ broj 2, str. 71-76, 2010. godine, Beograd*
- [42] J. Marku, K. Vaso, Optimization of copper slag waste content in blended cement production, *Časopis „Zaštita materijala“ broj 2, str. 77-80, 2010. godine, Beograd*
- [43] L. Xhagolli; E. Pinguli, E. Gjergjndreaj, Minimization of waste waters discharges from albanian breweries, *Časopis „Zaštita materijala“ broj 2, str. 81-86, 2010. godine, Beograd*
- [44] K. Vaso, M. Dema, Preparation of the anticorrosive paints with long oil alkyd resins modified with maleic anhydride and phthalic anhydride, *Časopis „Zaštita materijala“ broj 2, str. 87-93, 2010. godine, Beograd*